Available online at www.elixirpublishers.com (Elixir International Journal)

Chemical Engineering

Elixir Chem. Engg. 72 (2014) 25511-25515

ISSN: 2229-712X

Investigating the separation efficiency of Air-Water-Oil flow in a three phase pipe separator

Eyitayo A. Afolabi[1] and J.G.M Lee[2]

[1]Department of Chemical Engineering, Federal University of Technology, Minna, Nigeria.

[2]School of Chemical Engineering and Advanced Materials, Newcastle University, Newcastle upon Tyne, UK.

ARTICLE INFO

Article history:

Received: 29 March 2014;

Received in revised form:

19 June 2014;

Accepted: 3 July 2014;

Keywords

Separation efficiency,

Pipe separator,

Air-water-oil mixture,

Volume fraction.

ABSTRACT

The possibility of using a three phase pipe separator to separate a mixture of air-water oil was investigated. A 30 ID laboratory based pipe separator was designed, fabricated and installed to study the separation efficiency of air-water-oil mixture. A mixture of air-water-oil flow run through the pipe separator and the separation efficiency calculated in term of the percentage of clean water by volume at the water-rich outlet calculated. The results obtained showed that a clean water stream at the water-rich outlet of the pipe separator is achievable at high water volume fractions and low oil content. This confirmed the possibility that the three phase pipe separator can function as a free water knock-out device.

Introduction

Three-phase separations involve the separation of three-phase inlet stream into separate phases. That is, the removal of a combination of more than one phase from a continuous phase stream. A good example of the three phase separation is the separation of gas, oil and water using a three phase separator commonly referred to as free-water knockout vessel (Sayda and Taylor, 2007). In the past, the multiphase separation technology used in the oil and gas industry has been based on conventional vessel-type separators which are expensive, heavy and bulky in size. However, compact separators are now widely used as an effective and economical alternative to conventional separators especially in offshore platforms in oil and gas production operations. The compact separator is simpler to operate, more lightweight, has neither moving nor internal parts, requires less floor space, and involves lower capital and operational costs.

The compact separator often called a cyclone or pipe separator is a device that spins a continuous phase stream to remove entrained dispersed phases by centrifugal force. It has potential application as a free water knockout system in equipment for the upstream oil and gas production. This includes down-hole, surface (onshore and offshore) and subsea separation. The main application of the three phase cylindrical cyclone is to clean oily water for disposal by reducing oil concentrations to the order of parts per million in effluents.

Vasquez (2001) studied the separation efficiency of multiphase flow in a single stage 77-mm ID Gas-Liquid-Liquid Cylindrical Cyclone (GLLCC) separator. Air, water and oil were used as the test fluid and the superficial air velocity was kept constant in order to ensure a stratified flow pattern at the inclined inlet. Consequently, the flow pattern in the inlet did not vary. Experimental data for oil-water separation efficiency in the GLLCC were acquired for different combinations of the superficial oil and water velocities, and the location of the oil finder and split ratio were all varied for each combination. Vasquez (2001) showed that there is no good separation effect for an oil-dominated mixture as the swirl decays rapidly in the liquid section of the separator. At low liquid velocities, the flow in the inlet is found to be unstable due to churning in the vertical pipe that feeds the separator. As a result of these disturbances and a weak swirling effect, no oil core is formed and poor separation is obtained. However, at high liquid velocities a gas core is observed all the way through the liquid phase. This enables gas to be carried to the underflow, thereby limiting the gas-liquid separation. He concluded that the GLLCC is capable to provide a clean water stream in the water outlet pipe at low oil contents and high water superficial velocities. However, the cylindrical cyclone performs as a mixer rather than separator at high velocities.

A mechanistic model was developed by Vasquez (2001) for the prediction of air-oil-water separation performance of the GLLCC. The model consists of several sub-models such as inlet flow pattern analysis, nozzle analysis, droplet size distribution model and separation model based on droplet trajectories in swirling flow. The developed model was found capable of predicting both the trend of the experimental data as well as the absolute measured values. The main aim of this research is to determine the separation efficiency performance of air-oil-water mixture in a three phase pipe separator. Although, Vasquez (2001) carried out experimental investigation on a 77 mm ID three-phase cylindrical cyclone, this work is based on a 30 mm ID prototypes three phase pipe separator. In addition, the possibility of using CFD solver to determine the separation efficiency of the three phase flow in a pipe separator is hereby explored,

In recent years, the emergence of more powerful computers with large storage and high capacity processing facilities has provided the basis whereby computational fluid dynamics (CFD) can be used to predict flow pattern velocity profiles under a wide range of design and operating conditions. This has led to a better understanding of the turbulent flow behaviour in cyclones (Wilcox, 1993). There are several features of cyclone modelling that are essential in providing the opportunity for design modifications to achieve improved separation. These

Tele:

E-mail addresses: elizamos2001@yahoo.com

include detailed knowledge of the flow structure, the nature of air-core development and fluid- fluid and fluid-wall interactions. The Euler-Lagrange approach and the Euler-Euler approach are presently the major two approaches used to simulate the multiphase flows. The discrete phase model in ANSYS Fluent follows the Euler-Lagrange approach where the primary phase is treated as a continuum. However, the other phase (s) is dispersed in the flow field in the form of particles, bubbles or droplets. A fundamental assumption made in this approach is that the dispersed phase occupies a low volume fraction, which would suggest that the dispersed phase elements are not too close and should be treated as isolated (Crowe et al.,1998). The Euler-Euler approach is based on the assumption that the phases mix or separate, and that the dispersed phase occupies a high volume fraction (Cokljat et al., 2006; Crowe et- al.,1998). The high volume fraction suggests that the dispersed phase elements are too close to be treated as isolated. Therefore, the interaction between the multiphase flow and the effect of the secondary phase will be large enough to need accounting for.

Model Equations

Eulerian Multiphase Model

The phase-average continuity and momentum equations for the phase 'k' read;

$$\frac{\partial}{\partial t}(\bar{\alpha}_k\rho_k) + \nabla\left(\bar{\alpha}_k\rho_k\tilde{U}_k\right) = 0 \quad (1)$$

$$\frac{\partial}{\partial t}\left(\bar{\alpha}_k\rho_k\tilde{U}_k\right) + \nabla\left(\bar{\alpha}_k\rho_k\tilde{U}_k\otimes\tilde{U}_k\right) = -(\bar{\alpha}_k\nabla\bar{p}) + \nabla.\,\tilde{\tau}_k^t + [F_{DC} + F_{VM} + F_L] \quad (2)$$

The subscript '*k*' is replaced by '*c*' for continuous phase or '*d*' for dispersed phases. In addition, the laminar stress–strain tensor and other body forces (e.g., gravity) are omitted for the sake of simplicity. The tilde denotes phase-averaged variables, while the overbar refers to time-averaged values. The phase turbulent stress tensor embodies all fluctuations including the so-called pseudo-turbulence. The drag, virtual mass and lift forces are represented as F_{DC}, F_{VM} and F_L respectively. The drag force and virtual mass force between the continuous and dispersed phases are the only momentum exchange force considered and are defined as:

$$F_{DC} = K_{dc}\left[\left(\tilde{U}_d - \tilde{U}_c\right) - \left\{\frac{\overline{\alpha_d U_d'}}{\alpha_d} - \frac{\overline{\alpha_c U_c}}{\alpha_c}\right\}\right] \quad (3)$$

$$F_{VM} = 0.5\alpha_p\rho_q\left(\frac{d_q\vec{v}_q}{dt} - \frac{d_p\vec{v}_p}{dt}\right) \quad (4)$$

Here K_{dc} is a coefficient representing a characteristic density times an inverse time scale of the dispersed phase. The ANSYS FLUENT model assumes that the particle diameter is much smaller than the inter-particle spacing. Thus, the lift force is not considered negligible. In this study, Schiller-Nauman model (Schiller and Naumann, 1935) was used to calculate the fluid-fluid exchange coefficient. The time-averaged terms represent turbulent dispersion in the momentum equations. Turbulent stresses appearing in the momentum equations is defined by;

$$\tilde{\tau}_k^t = -\bar{\alpha}_k\rho_k\tilde{R}_{k,ij} \quad (5)$$

The Reynolds stresses need to be solves in order to close the phase-averaged momentum equations. The transport equation for the continuous phase Reynolds stresses in the case of the mixture turbulence model reads:

$$\frac{\partial}{\partial t}\left(\bar{\alpha}\rho\tilde{R}_{ij}\right) + \frac{\partial}{\partial x_k}\left(\bar{\alpha}\rho\tilde{U}_k\tilde{R}_{ij}\right) = -\bar{\alpha}\rho\left(\tilde{R}_{ik}\frac{\partial\tilde{U}_j}{\partial x_k} + \tilde{R}_{ik}\frac{\partial\tilde{U}_i}{\partial x_k}\right) + \frac{\partial}{\partial x_k}\left(\bar{\alpha}\mu\frac{\partial}{\partial x_k}\tilde{R}_{ij}\right) - \frac{\partial}{\partial x_k}\left[\overline{\bar{\alpha}\rho u_i' u_j' u_k'}\right] + \overline{\bar{\alpha}\rho}\left(\overline{\frac{\partial u_i'}{\partial x_j} + \frac{\partial u_j'}{\partial x_i}}\right) - \overline{\bar{\alpha}\rho\varepsilon_{ij}} \quad (6)$$

Discrete Particle Model

Particle Force Balance

By integrating the force balance on the particle, the trajectory of a discrete phase particle (or droplet or bubble) can be equated as the particle inertia with the forces acting on the particle. For the r direction in cylindrical coordinate, the force balance can be written in a Lagrangian reference frame as

$$\frac{du_p}{dt} = F_D\left(u - u_p\right) + \frac{g_x(\rho_p-\rho)}{\rho_p} + F_x \quad (6)$$

Where F_x is an additional acceleration term, $F_D\left(u - u_p\right)$ is the drag force per unit particle mass and

$$F_D = \frac{18\mu}{\rho_p d_p^2}\cdot\frac{C_D R_e}{24} \quad (7)$$

Here, *u* is the fluid phase velocity, u_p is the particle velocity, μ is the molecular viscosity of the fluid, ρ is the fluid density, ρ_p is the density of the particle, and d_p is the particle diameter. R_e is the relative Reynolds number, which is defined as

$$R_e \equiv \frac{\rho d_p|u_p-u|}{\mu} \quad (8)$$

Methodology

Experimental Facility and Flow Loop

The multiphase flow facility used in this study is based on one of the geometries developed for multiphase flow separation by the Separation Technology Project of the University of Tulsa, USA (Vasquez, 2001). It is an extension of the Gas-Liquid and Liquid-Liquid cylindrical cyclone technologies developed to separate gas-liquid-liquid mixtures. A 30 mm ID laboratory prototype pipe separator was fabricated and installed in the School of Chemical Engineering and Advanced Materials, Newcastle University, UK to study the separation efficiency of the pipe separator under different flow conditions at atmospheric pressure and room temperature (Afolabi and Lee, 2013). Detailed drawing of the pipe separator test section is given in Figure 1 and full description of the inlet configuration of the pipe separator is available in Afolabi (2012).

Separation Mechanism

The air-oil-water mixture enters through the inclined inlet designed to promote the pre-separation of the gas-liquid mixture. The tangential inlet with reduced area produces a swirling motion in the vertical cylindrical pipe. While the air flows upwards to the gas outlet and leaves the pipe separator, the liquid-liquid mixture moves to the lower section of the vertical pipe. As a result of differences in density, the centrifugal effect segregates the oil-water mixture, thereby concentrating the oil at the centre of the pipe whereas the water moves toward the wall region. The oil rich core formed at the centre flows through the oil finder and the water rich fraction flows to the annulus between the pipe wall and the oil finder, leaving the pipe separator through the water-rich outlet.

Air-Water-Oil Experiment

The experiments are performed using water (density 996 kg/m^3, viscosity 0.001 kg/ms); air (density 1.225 kg/m^3, viscosity 0.000018 kg/ms) and air (density 1.225 kg/m^3, viscosity 0.000018 kg/ms) at room temperature and atmospheric outlet pressure. Air, water and air are pumped from their respective storage tanks, metered and introduced to the pipe separator via a clear PVC schedule 40 pipe in-line mixer, which ensures minimum mixing. The mixture then flows through the inclined inlet to the pipe separator. The flow from the three outlets was controlled using natural rubber bungs to specify the split ratio as a function of mass flow rate passing through each outlet. Partially separated flow mixtures at the water, air and oil outlets were directed back into the partitioned water tank and air vented to the atmosphere.

A baffle was installed in the storage tank to separate oil from the partially separated mixture and siphon at the end of each experimental trial. Then after, the separated water passed through the 10mm baffle clearance to recirculate back to the water loop.

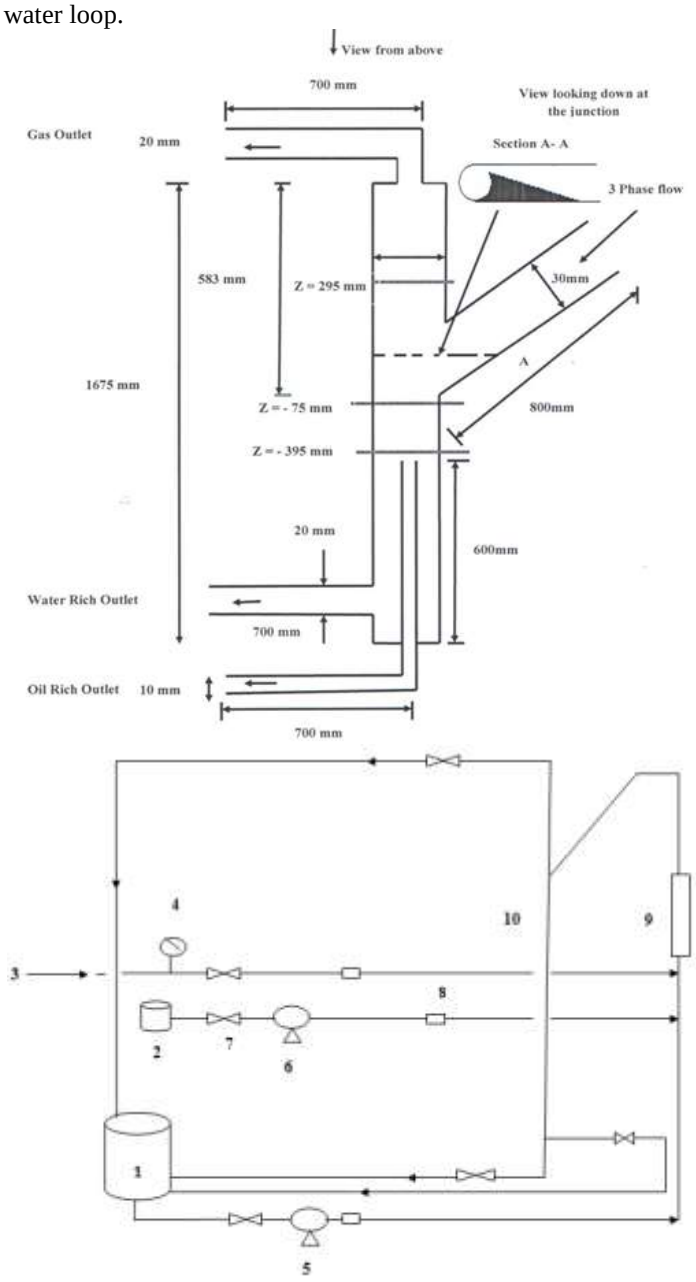

Figure 3.8: Diagram of the Air-Water-Oil Separation Experimental Flow Loop

1- Water tank,
2- Oil tank,
3- Air flow,
4-Pressure gauge,
5- Water pump,
6- Oil pump,
7-Valve,
8- Flow rate,
9- In line mixer,
10- Cylindrical cyclone

Preliminary investigations by Vazquez (2001) concluded that cylindrical cyclone achieves more efficient separation with stratified flow pattern at the inclined inlet. Therefore, this work considered stratified wavy flow pattern of air-water-oil mixture at the inclined inlet of the pipe separator. At atmospheric pressure and room temperature, a stratified wavy flow pattern at the inlet section of the separator was observed with air flow rate of 0.000045m^3/s. This air flow rate and corresponding water and oil flow rates shown in Table 1 with their associated properties such as densities, viscosities e.t.c, were then used to calculate and plot the Martinelli (X), and Taitel and Dukler (K) parameters onto the air-water flow map for inclined pipe (Perez, 2007; Barnea, 1987). These parameters were observed to lie in the stratified wavy region and confirmed a segregated flow pattern occurring at the inlet section of the pipe separator.

$$X = \sqrt{\frac{(\Delta P/_L)L}{(\Delta P/_G)G}} \quad (9)$$

$$K = \frac{U_G^2}{dgcos\alpha}\left(\frac{\rho_G}{\rho_G-\rho_L}\right)\left(\frac{\rho_L dU_L}{\mu_L}\right) \quad (10)$$

The separation efficiency experiments were carried out with varying water, oil flow rates and split ratio as shown in Tables 1 and 2.

Table 1: Experimental flow rates for air-water-oil flow

	A	B	C	
Water (10^{-5} m^3/s)	10.0 - 18.3	14.2	16.4	
Air (10^{-5} m^3/s)	4.5	4.5	4.5	
Oil (10^{-5} m^3/s)	1.8	0.25 – 5.5	0.83	

Table 2: Planned split ratio for the pipe separator outlets

	Split ratio
Water rich outlet	0.4
Air rich outlet	0.5
Oil rich outlet	0.1

Numerical simulation

The geometry of the pipe separator was created using the commercial software, Gambit and the numerical solution domain is with dimension of 0.885m, 1.82m and 0.646m in radial, axial and tangential direction respectively. An unstructured hybrid meshes with a total of 250,000 cells after grid independence study was generated and used for this work. Finite volume method with segregated 3D pressure based solver option and first order implicit unsteady state formulation was used for the numerical solution of the discretized equations.

At the inlet a "velocity inlet "boundary condition is applied and split ratios at the three outlets are specified. No-slip boundary condition is assumed at the internal wall. In the first stage, the Eulerian multiphase model in ANSYS-FLUENT was used to model the air-water multiphase flow in the pipe separator. An initial numerical solution was established using the standard $\boldsymbol{k-\varepsilon}$ model with the mixture model and was allowed to run for at least 5 seconds before switching to the Eulerian model. The multiphase version of the SIMPLE algorithm (Phase-Coupled SIMPLE) was used for pressure-velocity coupling. A transient solver with a 0.01 seconds time step and convergence criteria of at least 10^{-4} were used for the air-water simulations. In addition, the Reynolds Stress Model was used to capture the anisotropic features associated with the turbulent flow within the pipe separator.

The volume fraction of the oil dispersed phase was assumed to be very low such that each element of the oil droplets is not influenced by the neighbouring air-water phase. Hence, the Dispersed Phase Model (DPM) in ANSYS-FLUENT12.1 was used to track the dispersed oil droplets in the cyclone. Particle tracking, using the Lagrangian dispersed phase model is assumed to interact only with the primary phase and thereby neglected interactions between the disperse phases (Utikar et al., 2010; Crowe et al., 1998).

Results and Discussion

Figure 2 compares the percentage of water at the water-rich outlet as a function of water volume fraction at 4.5 x 10^{-5} m^3/s of air flow, 1.8 x 10^{-5} m^3/s of oil flow and the range of water flow is between 1.0 x 10^{-4} m^3/s to 1.83 x 10^{-4} m^3/s. Figure 3 shows a plot of the percentage of clean water at the water-rich outlet as a function of oil volume fraction at 4.5 x 10^{-5} m^3/s of air flow, 1.42 x 10^{-4} m^3/s of water flow and the range of oil flow is 2.5 x 10^{-6} m^3/s to 5.5 x 10^{-5} m^3/s. Figure 4 shows a plot of the percentage of clean water at the water-rich outlet against the split ratio at 4.5 x 10^{-5} m^3/s of air, 1.64 x 10^{-4} m^3/s of water and 8.3 x 10^{-6} m^3/s of oil flows. Figures 5 and 6 compare the measured and predicted separation efficiencies in term of the percentage of clean water passing through the water-rich outlet.

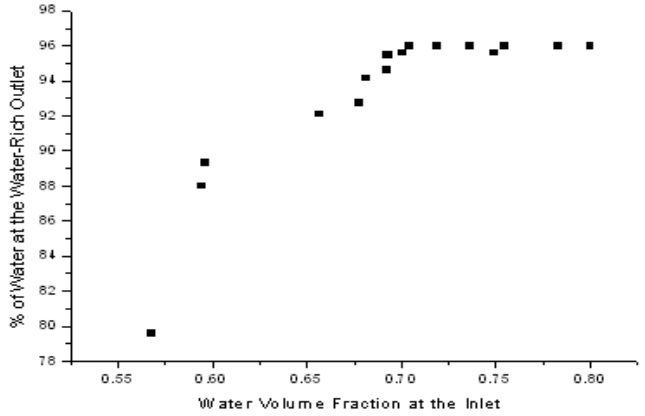

Figure 2: Percentage of Water at the Water-Rich Outlet against Water Volume Fraction

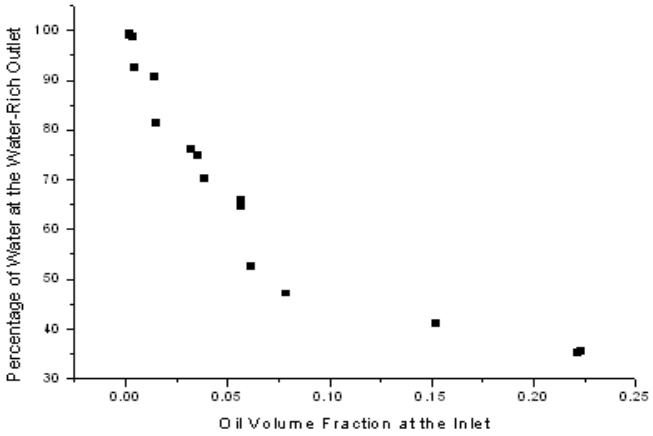

Figure 3: Percentage of Water at the Water-Rich Outlet against Oil Volume Fraction

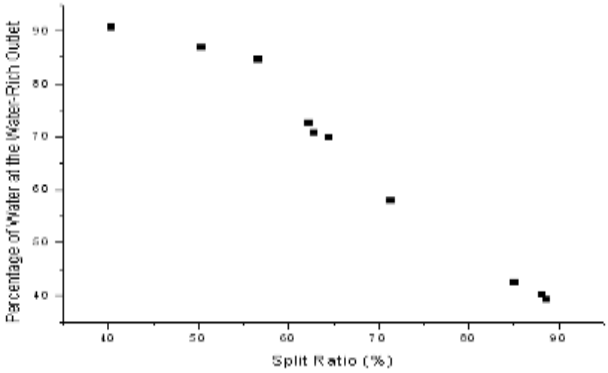

Figure 4: Plot of % Water Cut at the Water Outlet against Split Ratio

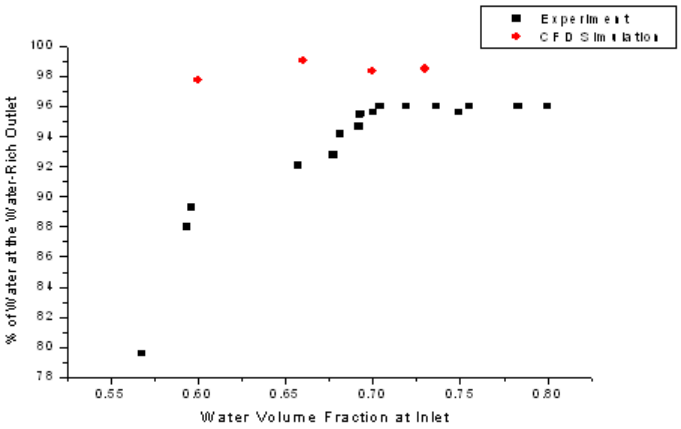

Figure 5: Comparison of the Percentage of Water at the Water Rich Outlet against Water Volume Fraction at the Inlet as Measured Experimentally and CFD Prediction

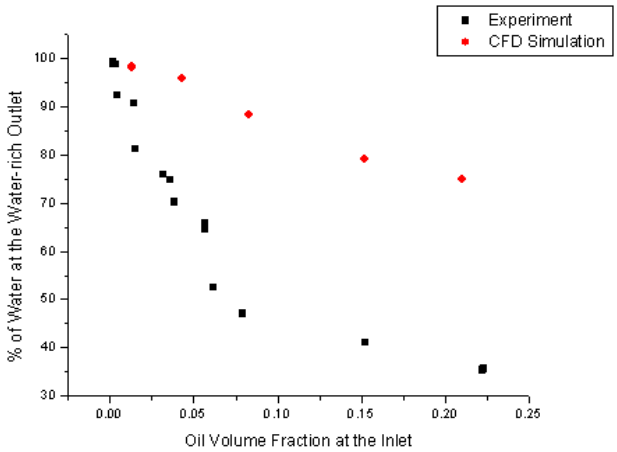

Figure 6: Comparison of the Percentage of Water at the Water Rich Outlet against Oil Volume Fraction at the Inlet as Measured Experimentally and CFD Prediction

Discussion

The results obtained in this work are presented in form of the percentage of clean water by volume at the water-rich outlet. This because, the primary objective of the pipe separator is to obtain a high purity of water through the water-rich outlet. The percentage clean water at the water-rich outlet is defined as the ratio of the volumetric flow rate of water to the total liquid volumetric flow rate at the water-rich outlet. In Figure 2, the percentage of clean water at the water-rich outlet increases as the water volume fraction increases.

It can be observed in Figure 3 that as oil volume fraction increases at the inlet section of the cyclone, the percentage of clean water at the water rich outlet decreases. From this plot, a volume fraction of less than or equal to 5% will give a good water purity at the water-rich outlet. A similar observation was made by Vasquez (2001), in which an estimated oil volume fraction of less than 10% was suggested as appropriate in order to ensure high separation efficiency.

The examination of Figure 4 reveals that an increase in the percentage of clean water at the water rich outlet is associated with a decrease in the split ratio. This means that increasing the split ratio beyond 55% leads to more of the dispersed oil droplets leaving with the water through the water-rich outlet. Figure 5 shows that the percentage of clean water at the water-rich outlet is observed to be over-predicted when compared with the experimental data. However, the capability of the pipe separator to produce clean water through the water-rich outlet is clearly indicated.

As shown in Figure 6, the measured and CFD profiles indicates that the percentage of water reduces with an increase in oil volume fraction at the inlet. However, there exist a large differences between the measured and CFD results. This deviation is strongly believed to be as a result of inherent drawbacks associated with Eulerian-Eulerian approach used for air-water simulation before tracking the oil droplets. For instance, bubble or droplet in the dispersed phase interacts only with the primary phase, neglecting the interactions between bubbles/droplets. This interaction causes coalescence and breakage that are proved to generate a considerate influence on the separation efficiency in the pipe separator (Utikar et al., 2010). The CFD models over-predicted the % of water at the water-rich outlet when compared with measured data by 2% - 9 % for the water-volume fraction and 8% - 95 % for the oil-volume fraction.

Conclusions

The separation efficiency of the air-water-oil flow was determined as a function of the clean water stream coming through the water rich outlet of the pipe separator. The possibility of the pipe separator producing clean water at the water-rich outlet has been demonstrated experimentally and numerically. It was observed that a clean water stream at the water-rich outlet of the pipe separator is achievable at high water volume fractions and low oil content. Therefore, this pipe separator is capable of functioning as a free water knock-out device.

References

Afolabi, E.A and Lee J.G.M (2013). Stereoscopic particle image velocimetry analysis of air-water flow in a pipe separator, *International Review of Chemical Engineering (IRECHE)*, 2013, Vol.5.N.3, 6-16.

Afolabi, E.A, *Experimental Investigation and CFD Simulation of Multiphase flow in a Three Phase Pipe Separator*, Ph.D Thesis, Newcastle University, UK, 2012.

Barnea, D. (1987) 'A unified model for predicting flow-pattern transitions for the whole range of pipe inclinations', *International Journal of Multiphase Flow*, 13, (1), pp. 1-12.

Cole-Parmer (2010) 'Technical Resource, Cole-Parmer Instrument Co. Ltd', London, UK.

Cokljat, D., Slack, M., Vasquez, S. A., Bakker, A. and Montante, G, Reynolds-stress model for Eulerian multiphase', *Progress in Computational Fluid Dynamics*, 2006, 6, (1-3), 168-178.

Crowe, C.S., M; Tsuji, Y (ed.) (1998) '*Multiphase flows with droplets and particles'* London CRC Press.

Garcia, J. C., Sierra, F. Z., Kubiak, J. and JuÃrez, D. (2003) 'Separating Three Phase Cyclones from the Rest', *Fluent News*.

Perez, Valente Hernandez; *Gas-liquid two-phase flow in inclined pipes* Ph.D dissertation, The University of Nottingham 2007

Sayda, A.F and Taylor, J.H (2007) 'Modeling and Control of Three-Phase Gravity Separators in Oil Production Facilities' American Control Conference, July 2007, pp.4847-4853.

Schiller, L. and Naumann, Z. (1935) 'Z. Ver. Deutsch. Ing', 77, pp. 318.

Utikar, R., Darmawan, H., Tade, M., Li, Q., Evans, G., Glenny, M. and Pareek, V. (eds.) (2010) '*Hydrodynamic Simulation of Cyclone Separators'* Computational Fluid Dynamics, Book edited by: Hyoung Woo OH, ISBN 978-953-7619-59-6, www.intechopen.com

Vazquez, C. O. (2001) *'Multiphase flow separation in Liquid-Liquid cylindrical cyclone and Gas-Liquid -Liquid cylindrical cyclone compact separators' T*hesis. The University of Tulsa.

Wilcox, D. C. (1993) '*Turbulence modeling for CFD'*. La Canada, DCW Industries Inc.